Hydrodynamic body shape analysis
and their impact on swimming performance

TIAN-ZENG LI, JIE-MIN ZHAN*

Department of Applied Mechanics and Engineering, Sun Yat-Sen University, Guangzhou, China.

This study presents the hydrodynamic characteristics of different adult male swimmer's body shape using computational fluid dynamics method. This simulation strategy is carried out by CFD fluent code with solving the 3D incompressible Navier–Stokes equations using the RNG k-ε turbulence closure. The water free surface is captured by the volume of fluid (VOF) method. A set of full body models, which is based on the anthropometrical characteristics of the most common male swimmers, is created by Computer Aided Industrial Design (CAID) software, Rhinoceros. The analysis of CFD results revealed that swimmer's body shape has a noticeable effect on the hydrodynamics performances. This explains why male swimmer with an inverted triangle body shape has good hydrodynamic characteristics for competitive swimming.

Key words: *swimming, biomechanics, swimmer's body shape, VOF method, numerical simulation*

1. Introduction

A V-shaped torso, which is one of the most sought-after physical builds that many men are keen to attain, makes the man look taller and more powerful. This body shape is usually called a swimmer's build as success in swimming. In general, an elite swimming athlete has the characteristics of the body with broad shoulders with stronger muscles, a great height, long arms, a thin waist, a long torso and powerful legs. This physique can offer powerful propulsion in swimming as reasonable distribution of the muscles. Actually, having a good body shape not only provides enough power for the propulsion but also makes the hydrodynamics characteristic advantageous for reducing the drag force in swimming. Here, we emphasize the effect of adult male swimmer's body shape on hydrodynamics characteristics in swimming.

Swimming performance depends on lots of comprehensive factors such as propulsive forces, drag forces, power output and swimming efficiency [6]. The segmental kinematics (segmental velocities, stroke rate, stroke length, stroke index) and technical skill level will have high correlation with the swimming efficiency [9]. Besides, an optimal swimmer's physique also plays an important role in reducing drag forces and improving swimming efficiency. Researchers have made several experimental attempts to examine the swimmer's physical characteristics to determine the characteristics of elite swimmers. Because the swimmers with different ages and genders have different physical characteristics, researchers hoped to use their research data to assess the relation between specific characteristics and performance for the different kinds of swimmers. Young swimmers became the focus of the research [7], [8], [23]. The findings could contribute to young swimmer's selection. The association of swimming performance with female's body composition was also addressed by the researchers [17]. These studies showed that endurance swimming was mildly associated with body adiposity. In addition, Wells [21] developed a comprehensive normative database of the physiological characteristics (descriptive characteristics, cardiovascular, respiratory, strength and power, body composition, and anthropometry) of elite swimmers to assess and identify the swimmer's physiological and talent in comparison with other populations.

However, few researchers have made a special study in analyzing the effect of swimmer's physique shape on swimming performance through hydrodynamics. Moreover, adopting experiment to investigate the physical characteristics of elite swimmers is inevitably involved with many complex and uneconomic difficulties. With the development of computer technology, computational fluid dynamics method was gradually applied to investigate competitive swimming for improving swimming performance [6], [3], [15]. In our current study, a numerical simulation strategy, which solves the 3D incompressible Navier–Stokes equations using the RNG k-ε turbulence closure, is presented for analyzing the hydrodynamics characteristic of different adult male swimmer's physique shape. The VOF method is used to track the complex free water surface. Full 3D body models are generated by Computer Aided Industrial Design (CAID) software, Rhinoceros. The analysis of CFD results revealed that swimmer's physiques has a noticeable effect on the hydrodynamics performances. An inverted triangle shaped torso is beneficial to improve swimming performances for a professional male athlete.

2. Materials and methods

2.1. Geometry

In many numerical analysis of human sports, laser scanning technique has been extensively used to obtain the precise 3D human model [2], [4]. Researchers first select a specific athlete and then operate the instrument to capture the corresponding human postures. However, for the quantitative analysis of the effect of swimmer's body shape on swimming performance, it may not be practical due to the difficulty of picking the appropriate
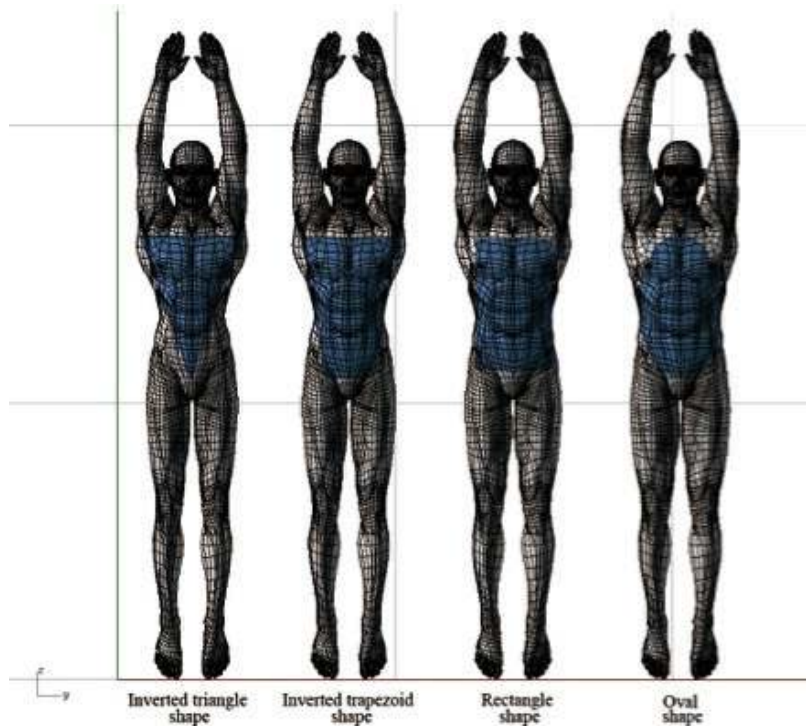

Fig. 1. Four 3D virtual models with different swimmer's physiques

Table 1. Some main parameters of the male swimmers

Parameters	Inverted triangle shape	Inverted trapezoid shape	Rectangle shape	Oval shape
Height (m)	1.82	1.82	1.82	1.82
Weight (Kg)	64	68	72	79
Bust (m)	1.02	1.04	1.06	1.08
Waist (m)	0.7	0.73	0.77	0.85
Hips (m)	0.85	0.87	0.89	0.96
Projected area (m^2)	0.109	0.113	0.122	0.131
Surface area (m^2)	1.894	1.929	1.999	2.053

swimmers for comparison. In our study, sets of 3D virtual human model based on the anthropometrical characteristics of the most common adult male swimmers are created by Computer Aided Industrial Design (CAID) software, Rhinoceros, with powerful model building capacity. Models of swimmer have respective physique shapes but height, being an inverted triangle, inverted trapezoid, rectangle, oval type body shape, respectively, as shown in Fig. 1, and some main parameters of male swimmers can be found in Table 1.

2.2. Computational domain and grid

In this simulation, swimmers are placed in the mid-line of a computational domain of 11.0 m in length and 6 m in width. The water depth of the flume is 1.8 m, the thickness of the air layer above the water surface is 1.2 m. The distance from the swimmer's hands to the velocity inlet is 2.61 m, while that of the

swimmer's toes to the outlet is 6.05 m. For simulating swimming near the water surface, the swimmer is towed with its longitudinal body axis at a depth of 0.2 m relative to the still water level.

Due to the complexity of the swimmer's geometry, a hybrid mesh method is adopted in the grid drawing process. Surfaces of swimmer are meshed by T-grid, then unstructured tetrahedral cells are generated around the body. And structured hexahedron cells are implemented in the rest of the computational domain. Additionally, local mesh encryption is carried out near the water surface for capturing the variation of the free surface, as shown in Fig. 2. In order to ensure grid dependence, a very high grid resolution is imposed close to the swimmer's surface based on the dimensionless wall unit y^*. The dimensionless wall unit is defined as the following equation

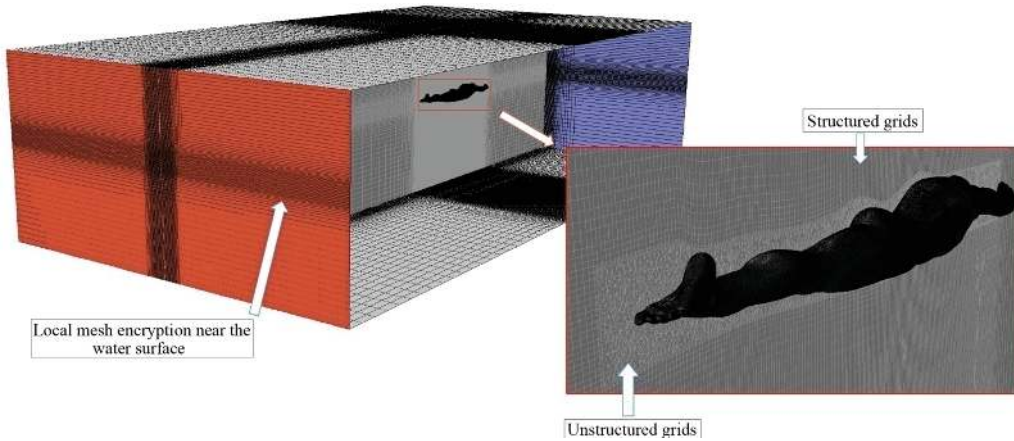$$y^* = \frac{\rho C_\mu^{1/4} k_p^{1/2} y_p}{\mu},\qquad(1)$$
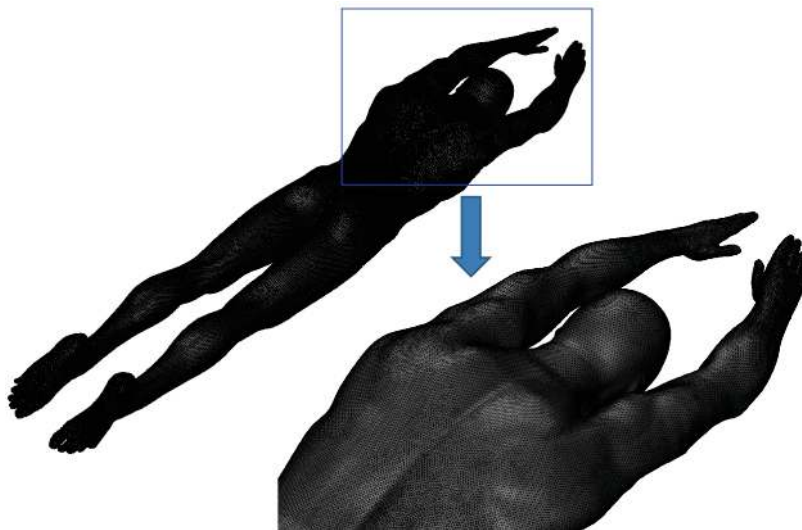

Fig. 2. Meshes of the computational domain

Fig. 3. Using the refined grids on swimmer's surface

where k_p is the turbulent kinetic energy at the near-wall node P; C_μ is a constant equal 0.09; y_p is the distance from point P to the wall; μ is the dynamic viscosity of the fluid. An appropriate value of y^* is from 30 to 300 based on the log-law for mean velocity under the standard wall functions [1]. In this study, for getting the optimal value of y^*, the fine cells of 0.001 m are used at the swimmer's surface, as shown in Fig. 3, and the total meshes of the computational domain are about 3,100,000.

2.3. Governing equations

The flow of this simulation is assumed as an incompressible, viscous fluid. It can be described by the Navier–Stokes equations and continuity equation as follows

$$\frac{\partial \rho}{\partial t} + \frac{\partial}{\partial x_i}(\rho u_i) = 0, \tag{2}$$

$$\frac{\partial}{\partial t}(\rho u_i) + \frac{\partial}{\partial x_j}(\rho u_i u_j)$$
$$= \frac{\partial p}{\partial x_i} + \rho g_i + \frac{\partial}{\partial x_j}\left(\mu \frac{\partial u_i}{\partial x_j}\right) + S_i, \tag{3}$$

where ρ is fluid density; $i, j = 1, 2, 3$ for three dimensional flows; u_i and u_j are the components of the velocity vector; p is the pressure; g_i is the component of acceleration due to gravity; μ is the viscosity; and S_i is the momentum source function.

The RNG k-ε turbulence model, which is based on renormalization-group (RNG) methods, has been widely used in many different engineering problems with the relatively high precision and reliability. This approach applies statistical methods to generate two new terms, turbulent kinetic energy k and dissipation rate ε. The two new turbulent variables can be obtained from the following transport equations

$$\frac{\partial k}{\partial t} + \frac{\partial}{\partial x_i}(k u_i) = \frac{\partial}{\partial x_j}\left(\alpha_k v_{eff} \frac{\partial k}{\partial x_j}\right) + G_k - \varepsilon, \tag{4}$$

$$\frac{\partial \varepsilon}{\partial t} + \frac{\partial}{\partial x_i}(\varepsilon u_i) = \frac{\partial}{\partial x_j}\left(\alpha_\varepsilon v_{eff} \frac{\partial \varepsilon}{\partial x_j}\right)$$
$$+ C_{1\varepsilon} \frac{\varepsilon}{k} G_k - C_{2\varepsilon} \frac{\varepsilon^2}{k}, \tag{5}$$

where v_{eff} is turbulent viscosity, G_k is the generation of turbulent kinetic energy due to the mean velocity gradients, $C_{1\varepsilon}$ and $C_{2\varepsilon}$ are constants equal 1.42 and 1.68, respectively.

In order to simulate swimmer gliding near the water surface more real, a two-phase flow including air and water is involved in this study. The Fluid of Volume (VOF) method is applied to track the deformation of the air–water interface. We used this approach successfully in a similar swimming study [22], demonstrating that the VOF method is capable of simulating swimming near the free surface. For the VOF method, a new transport equation for the volume fraction of fluid is introduced. F_q denotes the volume fraction and is determined by the following equations

$$\frac{\partial F_q}{\partial t} + \frac{\partial}{\partial x_i}(F_q u_i) = 0 \quad (q = 1, 2), \tag{6}$$

$$F_1 + F_2 = 1. \tag{7}$$

When $F_q = 1$, the cell is filled with the fluid of the q-th phase, in turn, for $F_q = 0$, the cell does not contain any fluid of the q-th phase. Additionally, for $0 < F_q < 1$, the cell is called an interface cell; $q = 1$ or 2 since there are only two phases, namely air and water.

The material properties (e.g., density or viscosity) appearing in the transport equations, φ, are evaluated by the following equation

$$\varphi = \varphi_1 F_1 + \varphi_2 F_2. \tag{8}$$

2.4. Boundary conditions

The boundary condition of this simulation is set based on a two-phase flow in a 3D flume with the top open to air. Water and air are specified by a free surface. Detailed boundary conditions adopted for our numerical simulations are as follows:

- The velocity inlet: a uniform constant horizontal speed is imposed ($z < 0$, water flows in; $z > 0$, air flows in, where z is vertical distance above the initial static water surface).
- The outlet: a pressure outlet condition is imposed ($p = \rho g h$, where p is hydrostatic pressure, h is water depth, density $\rho = 998.2$ kg/m^{-3} and acceleration due to gravity $g = 9.81$ ms^{-2}).
- The top: a pressure outlet condition is likewise imposed (all gradients are zero).
- The surface of the swimmer body and the walls of the flume: the no-slip condition is imposed (roughness is zero).

2.5. Numerical implementation

The simulation strategy with the 3D incompressible Navier–Stokes equations is solved by a commercial

computational fluid dynamics software, ANSYS FLUENT. The Pressure Staggering Option (PRESTO) discretization scheme is used for pressure. The Quadratic Upwind Interpolation of Convective Kinematics (QUICK) algorithm is used for the convection terms and the Pressure Implicit with Splitting of Operators (PISO) algorithm is used for the pressure-velocity coupling.

3. Results

3.1. Drag force

The hydrodynamic drag force F_D is the sum of the pressure drag F_p and friction drag F_f and then the non-dimensional corresponding drag coefficients are defined by the following equation

$$C_D = C_p + C_f = \frac{2F_D}{\rho U^2 A}$$

where C_D, C_p, C_f are the total drag force coefficients, pressure drag coefficient and friction drag coefficient, respectively ρ is the density of fluid. U is the towing velocity, and the projected area A is the area projected in the flow direction. In the present numerical simulation, friction drag can be calculated directly, and wave drag and form drag are subsumed under pressure drag. Detailed results of calculations for four sets of experiments are presented in Table 2.

In Fig. 4, variation of the pressure drag coefficient with flow velocity for four different swimmers is presented. It clearly shows that the swimmer with oval body shape gets the largest average pressure drag coefficient, and the pressure drag coefficient of the swimmer with the inverted triangle shape is smaller than those of other three swimmers. In addition, it is noted that the four swimmers can all get a relatively

Table 2. Drag force values at various velocity for swimming gliding near the water surface

| Speed (m/s)	Inverted triangle shape				Inverted trapezoid shape			
	Pressure force (N)	Skin friction (N)	Total force (N)	% Skin friction	Pressure force (N)	Skin friction (N)	Total force (N)	% Skin friction
1.2	20.5	4.66	25.16	18.50%	22.66	4.98	27.64	18.02%
1.4	24.65	6.06	30.71	19.73%	26.71	6.48	33.19	19.52%
1.6	36.66	8.02	44.68	17.95%	39.78	8.38	48.15	17.40%
1.8	45.41	9.94	55.35	17.96%	48.61	10.42	59.03	17.65%
2	54.66	12.17	66.83	18.21%	58.55	12.77	71.32	17.91%
2.2	67.33	14.55	81.88	17.77%	69.47	15.29	84.76	18.39%
Speed (m/s)	Rectangle shape				Oval shape			
	Pressure force (N)	Skin friction (N)	Total force (N)	% Skin friction	Pressure force (N)	Skin friction (N)	Total force (N)	% Skin friction
1.2	24.13	5.2	29.33	17.73%	27.39	5.58	32.97	16.94%
1.4	30.17	6.29	36.46	17.25%	32.69	7.23	39.92	18.11%
1.6	43.26	8.88	52.14	17.03%	47.59	9.56	57.15	16.73%
1.8	56.31	11.02	67.33	16.37%	63.34	11.91	75.25	15.83%
2	66.19	13.51	79.7	16.95%	75.73	14.5	90.25	16.07%
2.2	77.47	16.02	93.49	17.14%	86.54	17.08	103.62	16.48%
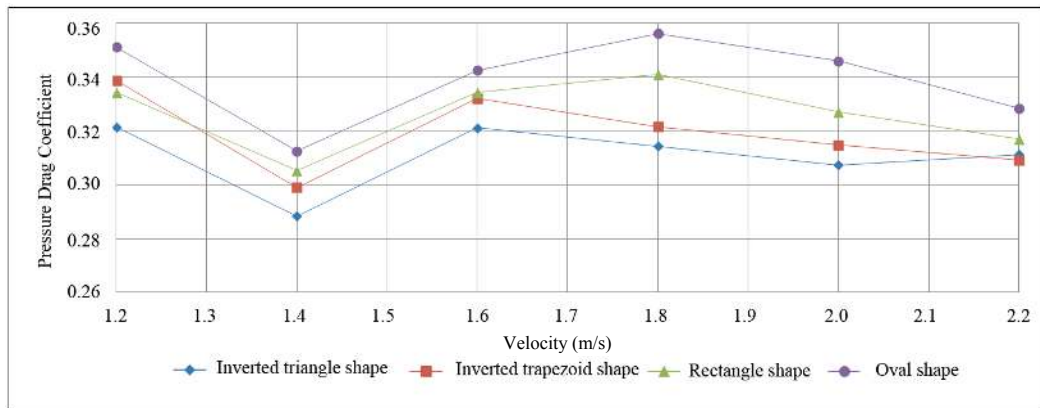
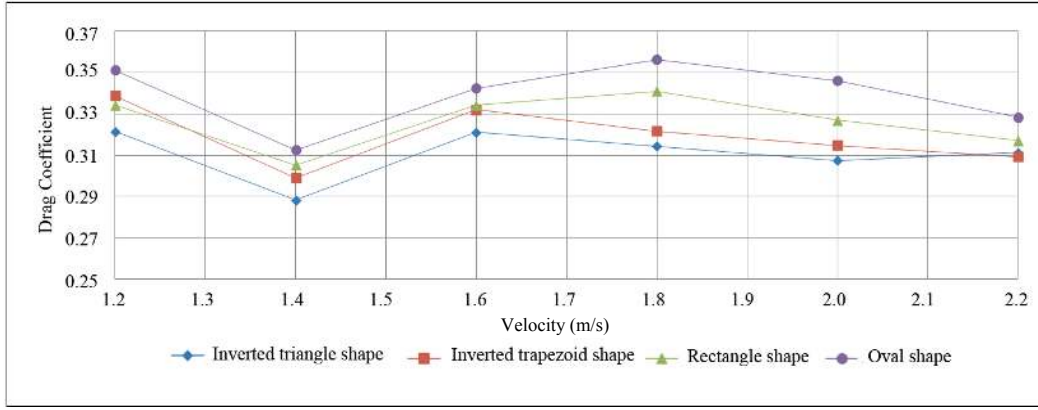Fig. 4. Pressure drag coefficient versus velocity for the different swimmers

Fig. 5. Total drag coefficient versus velocity for the different swimmers

smaller pressure drag coefficient at 1.4 m/s than other towing speeds. However, overall, the curves of the pressure drag coefficient for the four swimmers are relatively flat. Figure 5 shows the total drag coefficient versus velocity for the different swimmers. The trend of these curves is similar to those of the corresponding pressure drag coefficient. From Table 2, we can find the percentage of the total drag due to skin friction in different body shapes to be very similar with variation from 16.0% to 19.0% at inlet velocities from 1.2 m/s to 2.2 m/s from simulations. During gliding in swimming, the influence of body shape on skin friction is insignificant as far as swimming performance is concerned. The pressure drag is the decisive factor in analyzing the effect of body shape on drag force during gliding in swimming.

3.2. Visualization of flow field

In the experiment, observing the variation of the flow field around the swimmer is relatively difficult. However, in the numerical simulation, flow field can be straightforwardly visualized using post-process technique.

Figure 6a presents velocity streamlines around the upper body at 2.2 m/s for the four different swimmers. We can observe that evident vortexes are generated near to the swimmer's chin. We use the iso-surface of vorticity magnitude to further define the scale of these vortex zones, as shown in Fig. 6b. Similar vortex structures can also be found near to the swimmer's crotch in all the cases (see the right side of Fig. 7).

The velocity streamlines around the full body at $U = 2.2$ m/s for the four different swimmers are shown in Fig. 7. In this figure, wake flows behind the swimmers are different from each other. The swimmer with inverted triangle body shape has an optimal

streamline, while the swimmer with oval body shape gets a larger scale of wake flow zone. During swimming gliding near the water surface, the track of streamlines close to the water surface can also reflect the change of the water surface condition. From the figure (Fig. 8), waves are generated and form a wake behind the swimmer for all the cases. And we can observe the maximum deformation of the water surface in the case of swimmer with oval body shape, and the swimmer with inverted triangle body shape has got a relatively small deformation of the water surface. This is well agreed with the previous figure (Fig. 6).

4. Discussion

The aim of this study is to analyze the effect of different adult male swimmer's body shapes on hydrodynamic drag forces using numerical simulation. The results of calculations suggest that a male swimmer with an inverted triangle body shape has good hydrodynamic characteristics for competitive swimming.

Computational fluid dynamics methodology has been one of the best methods used for the analysis of fluid field in biomechanical engineering. Some relative work of swimming research has been verified by comparing the force drag between the CFD model and mannequin. Bixler [2] found the difference of the drag force between simulation and experiment to be within 4% during swimming gliding underwater. Zhan [22] carried out a 3D numerical simulation analysis of passive drag near free surface in swimming, and calculation results also agreed well with the mannequin tests.

As previously mentioned, the influence of body shape on skin friction is insignificant. Thus this article
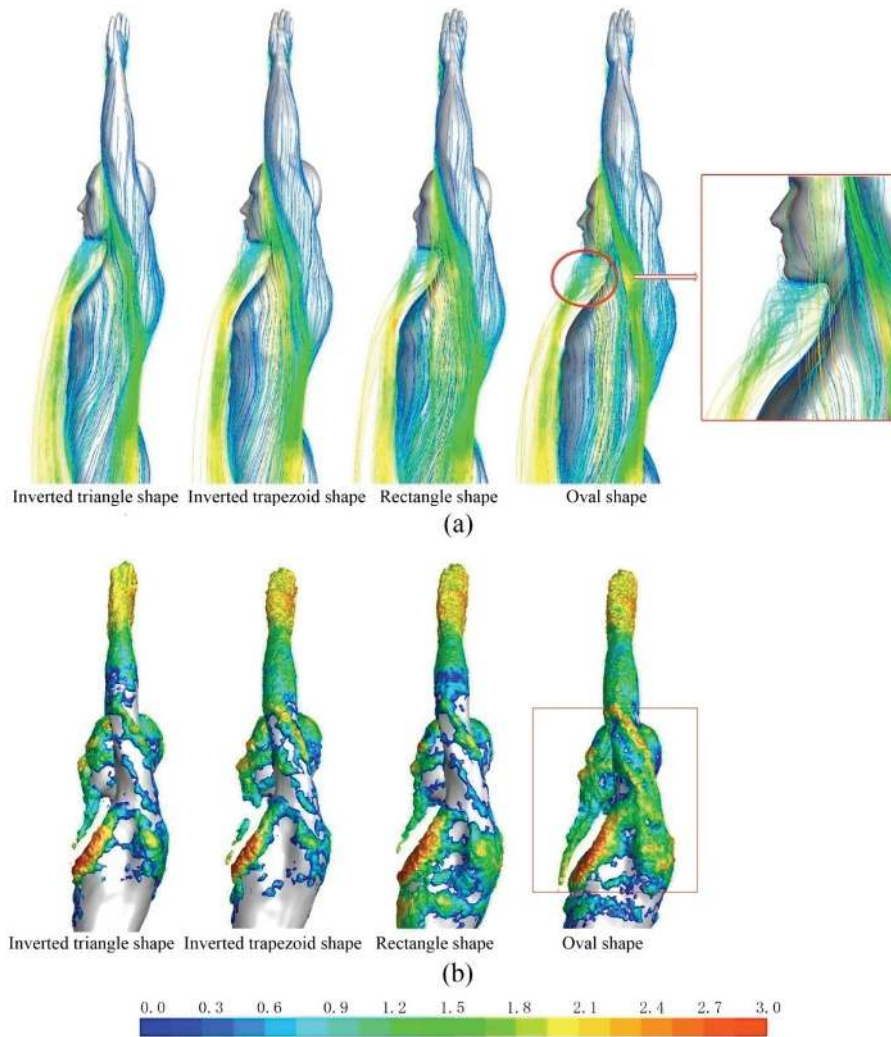
Fig. 6. (a) Velocity streamlines around the upper body at $U = 2.2$ m/s for the different swimmers. (b) Turbulent spot of the four swimmers at 2.2 m/s, visualized by iso-surface of vorticity magnitude (80 s^{-1}) and colored by velocity magnitude (m/s)
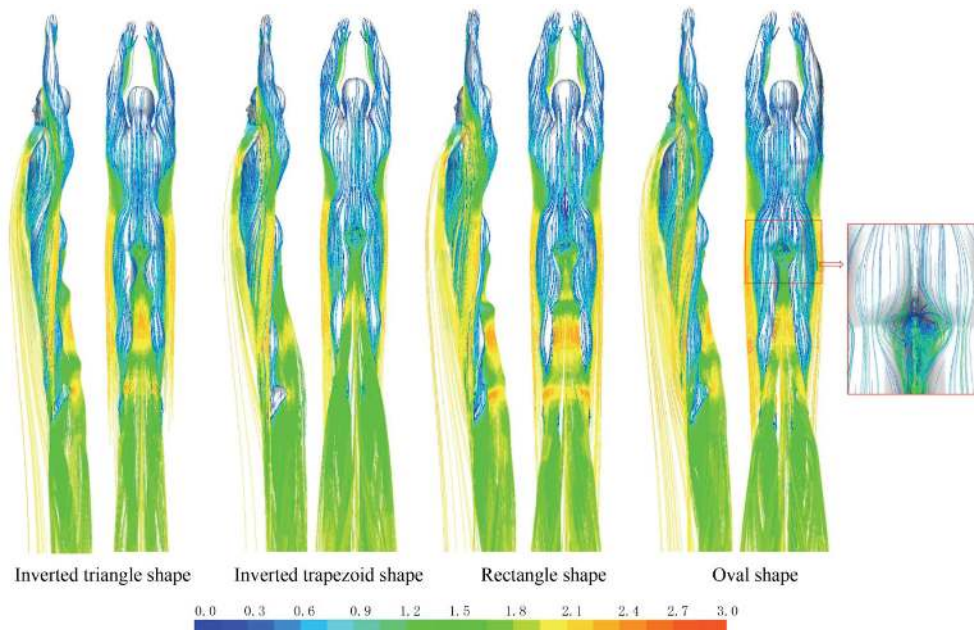

Fig. 7. Velocity streamlines around the full body at $U = 2.2$ m/s for different swimmers

mainly analyzes the effect of the pressure drag on swimming performance. There into, pressure drag is composed of two components: the form drag and wave drag. While swimming during gliding underwater, negative pressure gradients and turbulence zones are generated around swimmer's body because of the non-uniformity and complexity of the human body [11], which is the primary reason for adding form drag. Generally, such zones present complex surface geometries such as the head, shoulders, buttocks, heel and chest [5]. In summary, form drag that is directly related to body shape, and different body shape will cause different drag force. From the figure (Fig. 6), the scale of vortexes is most obvious in the swimmer with oval body shape, and those of the swimmer with inverted triangle body shape and the swimmer with inverted trapezoid shape are relatively weak. Vortices are an important source of the drag force and their strength should be reduced as much as possible. Figure 7 presents the velocity streamlines around the full body for different swimmers. We can observe that the swimmer with inverted triangle body shape has a better streamline than others. Actually, the inverted triangle body shape is closer to be a "drop of water" shape. From Vogel's [20] findings, the "drop of water" shape has a better hydrodynamic profile, reducing pressure gradient around the body. The "drop of water" shape keeps the boundary layer more time attached to the swimmer's body surface to delay the separation to a rear point of the body surface [13], it helps lower the hydrodynamic drag force for a swimmer.

Lyttle et al. [10] found that there was no significant wave drag contribution immersed at least 0.6 m. and Vennel et al. [19] also verified that wave drag on the mannequin was less than 5% of total drag for tows deeper than 0.5 m at 1 m/s and 0.7 m at 2 m/s. For the many previous studies [2], [14], swimmer is placed under water far away from the water surface, the wave drag is small enough at such a depth to be neglected in the calculation of the total drag. However, in the real swimming competition, swimmer gliding a deep underwater is not practical, which is unfavorable for emerging from the water surface to breath. During the near to the water surface, the wave drag will be generated [19], and the effect of the wave drag must be taken into account in the pressure drag. In this study, all cases are conducted at a depth of 0.2 m relative to the still water level. Actually, it is difficult to directly divide pressure drag into form drag and wave drag for swimming near the water surface. A similar difficulty also occurs in model testing of ships, where wave drag is usually isolated by calculations based on Michell's [12] theory for slender ships [16], a technique verified by measurements of the wave pattern behind models [5]. Here, we analyze the characteristics of the wave drag with the help of the visualization of computational simulation. Figure 8 presents the deformation of the free surface for the different swimmers. It can be observed that swimmer with inverted triangle body shape has got a relatively small deformation of the water surface. In general, the less the water surface deforms, the less the wave drag adds. Thus, we can conclude that the swimmer with inverted triangle

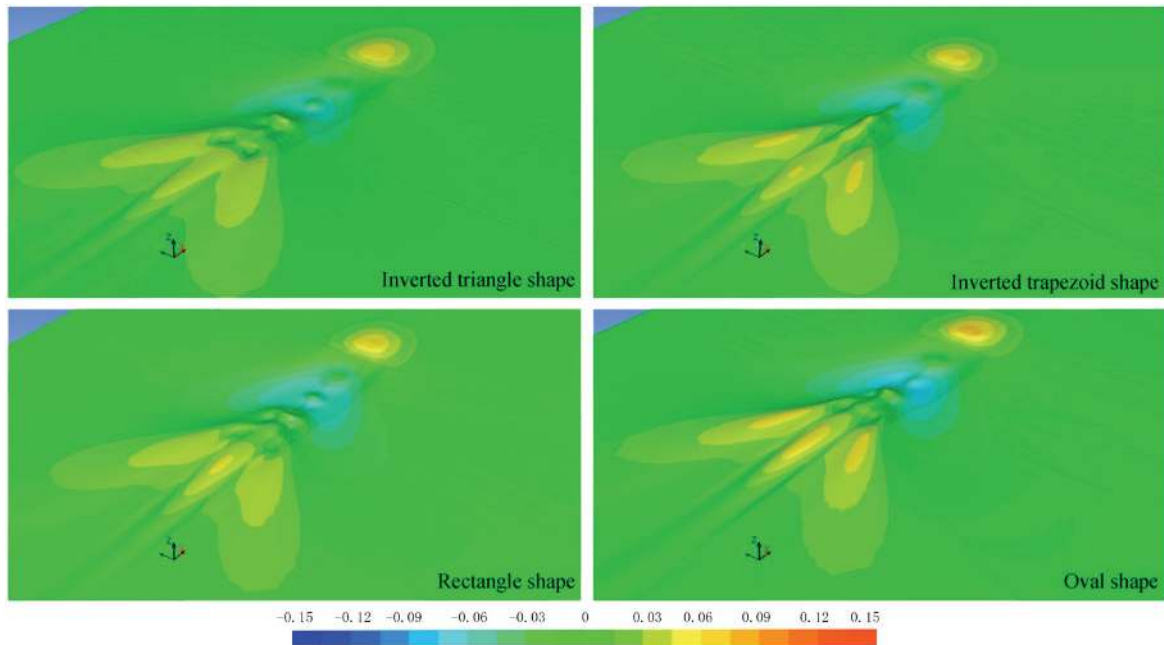-0.15   -0.12   -0.09   -0.06   -0.03   0   0.03   0.06   0.09   0.12   0.15

Fig. 8. Deformation of the free surface for the different swimmers, colored by the Z coordinate (m)

body shape gets the smallest wave drag compared to other three swimmers.

5. Conclusion

A set of numerical 3D full-body models for swimming based on the Navier–Stokes equations and the VOF method has been established. Hydrodynamic characteristics of four adult male swimmers with different body shapes have been analyzed. A vivid visualization of computational results reveals that the male swimmer with inverted triangle body shape has an optimal hydrodynamic characteristics in swimming. Our results suggest that one of the conditions for coaches to pick out the potential male swimmer is that the candidate should have an inverted triangle body shape. On the other hand, for keeping favorable performance, male athletes should keep prefect shape like the inverted triangle through healthy eating and body-building.

Acknowledgement

References

[1] ANSYS INC., ANSYS Fluent 12.0 theory guide, 2009.

[2] BIXLER B., PEASE D., FAIRHURST F., *The accuracy of computational fluid dynamics analysis of the passive drag of a male swimmer*, Sport Biomech., 2007, Vol. 6, 81–98.

[3] BIXLER B., SCHLODER M., *Computational fluid dynamics: An analytical tool for the 21st century swimming scientist*, J. Swim. Res., 1996, Vol. 11, 4–22.

[4] BLOCKEN B., DEFRAEYE T., KONINCKX E., CARMELIET C., HESPEL P., *CFD simulations of the aerodynamic drag of two drafting cyclists*, Comput. Fluids, 2013, Vol. 71, 435–445.

[5] CLARYS J.P., *Human morphology and hydrodynamics*, J. Terauds & E.W. Bedingfield, 1979.

[6] COHEN R.C.Z., CLEARY P.W., MASON B., *Improving Understanding of Human Swimming Using Smoothed Particle Hydrodynamics*, Proceedings of 2010 Singapore IFMBE, 6th World Congress of Biomechanics (WCB 2010), 2010, Vol. 31, 174–177.

[7] GELADAS N.D., NASSIS G.P., PAVLICEVIC S., *Somatic and physical traits affecting sprint swimming performance in young swimmers*, Int. J. Sports Med., 2005, Vol. 26, 139–144.

[8] JÜRIMÄE J., HALJASTE K., CICCHELLA A., LÄTT E., PURGE P., LEPPIK A., JÜRIMÄE T., *Analysis of swimming performance from physical, physiological and biomechanical parameters in young swimmers*, Pediatr. Exerc. Sci., 2007, Vol. 19, 70–81.

[9] KUCIA-CZYSZCZOŃ K., DYBIŃSKA E., AMBROŻY T., CHWAŁA W., *Factors determining swimming efficiency observed in less skilled swimmers*, Acta Bioeng. Biomech., 2013, Vol. 15, 115–124.

[10] LYTTLE A.D., BLANKSBY B.A., ELLIOTT B.C., LLOYD D.G., *Optimal depth for streamlined gliding*, Keskinen K.L., Komi P.V., Hollander A.P., 1999.

[11] LYTTLE A.D., *Hydrodynamics of the Human Body During the Freestyle Tumble Turn*, PhD Thesis, The University of Western Australia, Nedlands, Australia, 1999.

[12] MICHELL J.H., *The wave-resistance of a ship*, The Philosophical Magazine, 1898, Vol. 45, 106–123.

[13] POLIDORI G., TAIAR R., FOHANNO S., MAI TH., LODINI A., *Skin-friction drag analysis from the forced convection modeling in simplified underwater swimming*, J. Biomech., 2006, Vol. 39, 2535–2541.

[14] POPA C.V., ARFAOUI A., FOHANNO S., TAÏAR R., POLIDORI G., *Influence of a postural change of the swimmer's head in hydrodynamic performances using 3D CFD*, Comput. Method. Biomech., 2012, Vol. 17, 344–351.

[15] ROUBOA A., SILVA A., LEAL L., ROCHA J., ALVES F., *The effect of swimmer's hand/forearm acceleration on propulsive forces generation using computational fluid dynamics*, J. Biomech., 2006, Vol. 39, 1239–1248.

[16] TUCK E.O., *The wave resistance formula of J.H. Michell (1898) and its significance to recent research in ship hydrodynamics*, J. Aust. Math. Soc. B., 1989, Vol. 30, 365–377.

[17] TUURI G., LOFTIN M., OESCHER J., *Association of swim distance and age with body composition in adult female swimmers*, Med. Sci. Sports. Exer., 2002, Vol. 34, 2110–2114.

[18] VAN MANEN J.D., VAN OOSSANEN P., *Resistance*, Lewis E., 1988.

[19] VENNEL R., PEASE D., WILSON D., *Wave drag in human swimmers*, J. Biomech., 2006, Vol. 39, 664–671.

[20] VOGEL S., *Life in moving fluids. The Physical Biology of Flow*, Princeton University Press, Princeton, 1994.

[21] WELLS G., SCHNEIDERMAN-WAKER J., PLYLEY M., *Normal physiological characteristics of elite swiixirners*, Pediatr. Exer. Sci., 2006, Vol. 18, 23–30.

[22] ZHAN J.M., LI T.Z., CHEN X.B., LI Y.S., ONYX WAI W.H., *3D numerical simulation analysis of passive drag near free surface in swimming*, China Ocean Eng., 2014, Vol. 29(2), DOI: 10.1007/s13344-014-0080-x

[23] ZUNIGA J., HOUSH T.J., MIELKE M., HENDRIX C.R., CAMIC C.L., JOHINSON G.O., HOUSH D.J., SCHMIDT R.J., *Gender comparisons of anthropometric characteristics of young sprint swimmers*, J. Strength Cond. Res., 2011, Vol. 25, 103–108.